Modelling Wave Interaction with Porous Structures using Boussinesq Equations

Shagun Agarwal, V Sriram, and K Murali

Indian Institute of Technology Madras, Chennai, India
shagun.1994@gmail.com

Abstract. The paper presents a numerical model of the two - dimensional enhanced Boussinesq equations to simulate wave transformations in the near-shore region. The finite element based discretization over unstructured mesh with triangular elements uses mixed linear and quadratic shape functions. The domain integrals are calculated analytically. The model is extended to study flow through porous structures using Darcy velocity, with the energy dissipation within the porous medium modelled through additional laminar and turbulent resistance terms. A single set of empirical constants gives accurate prediction for various stone sizes and porosity. This paper reports the model development and its validation using existing experimental studies. Application of the model is demonstrated by studying the interaction between ship generated waves in a narrow channel and the porous walls of the channel.

Manuscript accepted in Proceedings of the Fourth International Conference in Ocean Engineering (ICOE2018)
Published version at https://doi.org/10.1007/978-981-13-3119-0_35

Cite as : Agarwal, S., Sriram, V., Murali, K. (2019). Modelling Wave Interaction with Porous Structures Using Boussinesq Equations. In Proceedings of the Fourth International Conference in Ocean Engineering (ICOE2018) (pp. 573–583). Springer. https://doi.org/10.1007/978-981-13-3119-0_35

Keywords: Boussinesq equation, porous structure wave interaction

1 Introduction

Boussinesq type equations are widely used for modelling wave transformations in near shore region. The increasing use of this equations stem from the fact that it reduces the three dimensional potential flow problems to a two dimensional problem based on depth-averaged velocity, thus reducing the computational cost drastically in modelling the large domain while capturing the important phenomenon. Early formulations based on depth averaged velocities were linear and limited to shallow water regions. Modifications in [1] extended it to intermediate water depths. Further non-linear improvements in [2,3] saw practical use in coastal engineering problems.

Wave interaction with porous structures, like rubble mound breakwater and sea wall, is an important phenomenon for coastal engineering. Their partially reflecting nature is favourable in dissipating wave energy. A comprehensive wave model should incorporate porous structure interaction for practical application. A comparison of different porous flow

equations was done in [4,5]. Early diffraction around porous breakwater model by [6] was limited to thin breakwater. A rigorous comparison with experiment results on transmission and reflection of solitary wave was done in [7]. Some notable Boussinesq models based on Darcy porous flow equation are [8,9].

This work presents a finite element based numerical model of Boussinesq equation with mixed spatial interpolation, covering shallow to intermediate water depth regions. Interaction with porous structure is modelled using Darcy velocity along with linear and turbulent resistance terms. The basic model is validated using experimental results from standard Berkhoff shoal test. The porous flow model is validated through results on reflection and transmission coefficients for porous breakwater. A potential application of the model is presented by studying interaction of ship generated waves in a narrow channel with its partially reflecting walls.

2 Governing Equations

This work uses enhanced Boussinesq equations as derived in [1], which is valid for slowly varying bathymetry and incorporates linear dispersion characteristics. They are evaluated in depth integrated form, with P and Q as depth integrated velocity flux along x and y Cartesian coordinates axes respectively, η as water surface elevation, h as still water-depth, $d = h + \eta$ as total water-depth, g as acceleration due to gravity and ρ as density of water.

The enhanced Boussinesq terms Ψ_x and Ψ_y as defined in [1] involve third order spatial derivatives of surface elevation. A linear shape function for η estimation in finite element would not be able to calculate this higher order derivative. Therefore an auxiliary variable w was introduced in [10] as defined by Eq 1. This work uses these modified Boussinesq equations as a basis for deriving the flow equation through porous medium.

$$w = \frac{\partial}{\partial x}\left(h\frac{\partial \eta}{\partial x}\right) + \frac{\partial}{\partial y}\left(h\frac{\partial \eta}{\partial y}\right) \tag{1}$$

Flow in a porous medium of porosity λ is modelled using the Darcy velocity or seepage velocity. If P_d is the depth integrated Darcy flux, then

$$P_d = \lambda P \implies P = \frac{P_d}{\lambda} \tag{2}$$

The energy dissipation inside the porous medium is modelled using the laminar and turbulent drag resistance terms, $f_l u$ and $f_t|u|u$; where f_l and f_t are the respective coefficients and are obtained using the empirical relations from [11].

$$f_l = \alpha_0 \frac{(1-\lambda)^3}{\lambda^2}\frac{\nu}{s^2} \qquad f_t = \beta_0 \frac{(1-\lambda)}{\lambda^3}\frac{1}{s} \tag{3a}$$

where ν is the kinematic viscosity of water, s is the characteristic size of the stone and α_0 and β_0 are empirical constant with recommended range of 780 - 1500 and 1.8 - 3.6 respectively. The final form of the Boussinesq equations for flow through porous medium is given in Eq 4. This is used for the final finite element formulation. Putting $\lambda = 1$ makes $f_l = 0$ and $f_t = 0$

thus returning them to the original form as in [10].

$$\frac{\partial \eta}{\partial t} + \frac{\partial}{\partial x}\left(\frac{P}{\lambda}\right) + \frac{\partial}{\partial y}\left(\frac{Q}{\lambda}\right) = 0 \tag{4a}$$

$$\frac{\partial P}{\partial t} + \frac{\partial}{\partial x}\left(\frac{P^2}{\lambda d}\right) + \frac{\partial}{\partial y}\left(\frac{PQ}{\lambda d}\right) + \lambda g d\frac{\partial \eta}{\partial x} + \lambda f_l P + \lambda f_t \frac{P}{d}\sqrt{P^2+Q^2} + \Psi'_x = 0 \tag{4b}$$

$$\frac{\partial Q}{\partial t} + \frac{\partial}{\partial x}\left(\frac{PQ}{\lambda d}\right) + \frac{\partial}{\partial y}\left(\frac{Q^2}{\lambda d}\right) + \lambda g d\frac{\partial \eta}{\partial y} + \lambda f_l Q + \lambda f_t \frac{Q}{d}\sqrt{P^2+Q^2} + \Psi'_y = 0 \tag{4c}$$

with the Boussinesq terms Ψ'_x and Ψ'_y given by

$$\begin{aligned}\Psi'_x = -\left(B+\frac{1}{3}\right)h^2\left(\frac{\partial^3 P}{\partial x^2 t} + \frac{\partial^3 Q}{\partial xyt}\right) - h\frac{\partial h}{\partial x}\left(\frac{1}{3}\frac{\partial^2 P}{\partial xt} + \frac{1}{6}\frac{\partial^2 Q}{\partial yt}\right) \\ -h\frac{\partial h}{\partial y}\left(\frac{1}{6}\frac{\partial^2 Q}{\partial xt}\right) - \lambda B g h^2 \frac{\partial w}{\partial x}\end{aligned} \tag{5a}$$

$$\begin{aligned}\Psi'_y = -(B+\frac{1}{3})h^2\left(\frac{\partial^3 P}{\partial xyt} + \frac{\partial^3 Q}{\partial y^2 t}\right) - h\frac{\partial h}{\partial y}\left(\frac{1}{6}\frac{\partial^2 P}{\partial xt} + \frac{1}{3}\frac{\partial^2 Q}{\partial yt}\right) \\ -h\frac{\partial h}{\partial x}\left(\frac{1}{6}\frac{\partial^2 P}{\partial yt}\right) - \lambda B g h^2 \frac{\partial w}{\partial y}\end{aligned} \tag{5b}$$

3 Numerical Formulation

The finite element formulation is done using standard Galerkin method. The two-dimensional computational domain is meshed with irregular triangles. Each triangular element consists of 6 nodes; 3 vertices and middle points of each side. The variable P and Q are evaluated on the 6 nodes and interpolated using quadratic shape function ϕ to handle high order derivatives in Eq 4. The variables η and w are evaluated on the 3 vertices of each triangle and interpolated using linear shape function δ. The derivatives of the unknowns are evaluated using the Jacobian matrix and standard triangle element. The governing equations are converted to integral form using δ_i as trial function for Eq 1 and Eq 4a; and ϕ_i as trial function for Eq 4b and Eq 4c. Certain higher order derivatives are converted to weak form using Gauss divergence theorem. The integration was carried out analytically over a standard triangular element and then scaled using the Jacobian. This avoids the approximations of Gauss quadrature method and involves lesser computation. The discretised weak form of governing equations is given in Eq 6 using matrix notation. The definition of each matrix in Eq 6 is excluded from this manuscript.

$$M_2 w = f_w - D\eta \tag{6a}$$

$$M_2 \dot{\eta} = C_x P + C_y Q \tag{6b}$$

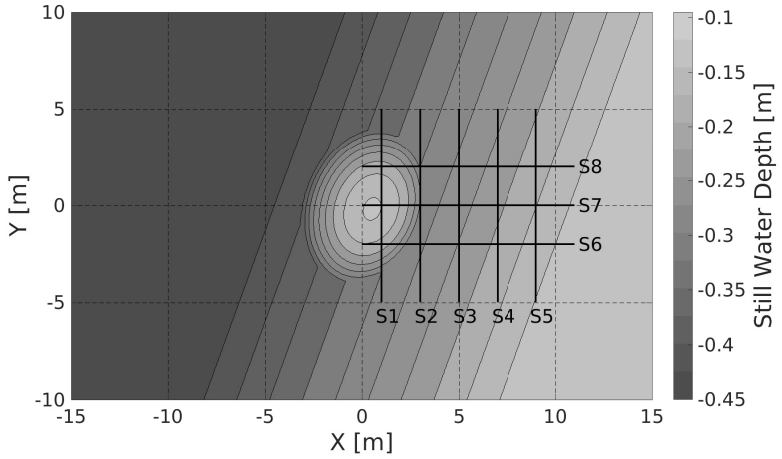

Fig. 1. Contour plot of Berkhoff shoal bathymetry; measurements along lines (- - -)

$$\begin{bmatrix} M_1 + B_1 & B_2 \\ B_3 & M_1 + B_4 \end{bmatrix} \begin{bmatrix} \dot{P} \\ \dot{Q} \end{bmatrix} = \begin{bmatrix} f_{p1} & f_{p2} & f_{p3} \\ f_{q1} & f_{q2} & f_{q3} \end{bmatrix} \begin{bmatrix} \dot{P} \\ \dot{Q} \\ w \end{bmatrix} - \begin{bmatrix} B_5 \\ B_6 \end{bmatrix} w$$
$$- \begin{bmatrix} N + R_l & 0 & G_x \\ 0 & N + R_l & G_y \end{bmatrix} \begin{bmatrix} P \\ Q \\ \eta \end{bmatrix} - \begin{bmatrix} R_{tx} \\ R_{ty} \end{bmatrix} \sqrt{P^2 + Q^2} \tag{6c}$$

$\dot{P}$, $\dot{Q}$ and $\dot{\eta}$ denote the time derivatives. The time integration is done using explicit 3 point Adams-Bashforth method. The algebraic equations 6 are of form $AX = B$. The solution for the unknown X is obtained using iterative-type GMRES solver using PARALUTION library [12] with OpenMP based parallel implementation. There are four types of boundary conditions that are modelled — fully reflection slip wall, fully reflecting no-slip wall, inlet boundary condition and absorbing layer boundary condition. The Dirichlet type boundary conditions are implemented using penalty method [13, ch.4] and Neumann type boundary conditions are applied using iterative method. Finally the absorbing layer boundary condition is applied using a sponge layer.

4 Numerical Experiments

4.1 Regular Waves Over Berkhoff Shoal

Berkhoff shoal bathymetry is widely used to validate numerical models on surface waves. The bathymetry is a constant $1 : 50$ slope with water depth range of $0.1m$ to $0.45m$. It consists of an elliptical shoal with the centre at a distance of $5.84m$ from the shoal toe, with $4m$ major and 3 minor axis. The depth contours are aligned at an angle of 20^0 to the incident regular waves. The computational domain is of size $36m \times 20m$ with the origin located at the centre of the ellipse. The analytical expression for this bathymetry can be found in [14].

The wave inlet boundary is located at side $x = -15m$, generating regular waves of period $1s$ and heigh $0.0464m$. The sides $y = \pm 10m$ are fully reflecting slip walls. A $6m$ sponge layer is located at side $x = 15m$ to absorb the waves.

The irregular mesh implementation allows use of variable mesh size. The region between $x = -8m$ and $x = 15m$ is meshed with mean element area of $0.005m^2$, and the remaining space has element area of $0.02m^2$. The mesh has 97062 elements with 48915 linear nodes and 194891 total nodes. Simulation time step is $0.005s$, obtained after time convergence study. The simulated time is $40s$.

The results from this simulation are compared with experimental wave height measurements from [15] in Fig 2. The figure also shows comparison with numerical results obtained using FUNWAVE 1.0 [16] with similar mesh characteristics. The measurements are made along the line sections S1-S8, as shown in Fig 1. The model correctly captures the location and magnitude of peaks in the wave-height along the line sections, thus validating the implementation of the numerical model.

4.2 Flow of Solitary Wave through Porous Breakwater

The numerical modelling of flows through porous structures is verified through the study of interaction of solitary wave with porous breakwater. Solitary waves are non-dispersive in nature and can keep a constant elevation profile over a long distance of propagation. The solitary wave profile with wave-height (H) at water depth (h) used in the present study is given in [17].

$$\eta(x,t) = Hsech^2[\kappa(Ct - X_0)] \qquad \kappa = \sqrt{\frac{3H}{4h^3}} \qquad C = \sqrt{g(h+H)} \tag{7}$$

with the depth integrated velocity profile given by

$$P(x,t) = CHsech^2[\kappa(Ct - X_0)] \tag{8}$$

The governing equations for this model are weakly non linear and hence will not be able to match the conventional non-linear initial condition for solitary wave. To obtain a constant profile, the solitary wave is first allowed to propagate for long distance at a constant water depth. At the beginning of these computations, the wave height and shape keep changing. But over some distance of propagation the solitary wave achieves a stable shape and is then used for the study of interaction with porous breakwater. This is similar to te approach taken in [2].

The computational domain is $10m \times 2m$. A uniform element size of $0.05m$ and time-step of $0.005s$ is used for all cases. The breakwater is located in the middle of the domain. Porosity of the gravel is taken as 50% with drag resistance coefficients $\alpha = 1100$ and $\beta = 1.50$. Two sizes of irregular gravel are studied with median diameter $1.6cm$ and $2.0cm$. Width of breakwater are taken as $15cm$ and $30cm$. The water depth is kept constant at $0.1m$ and wave heights are in the range of $0.01m$ to $0.035m$.

As shown in Fig 3, the solitary wave on hitting the breakwater splits into two parts, and is partly reflected and transmitted. The heights of these two waves are non-dimensionalised using the initial wave height to obtain the reflection and transmission coefficients (ζ_R, ζ_T), which are used to compare the results with reference studies. Fig 4 shows comparison of results from present work with numerical and experimental results from [7] (using $\alpha = 1100$ and $\beta = 0.81$) for different gravel sizes and breakwater widths. The present model can

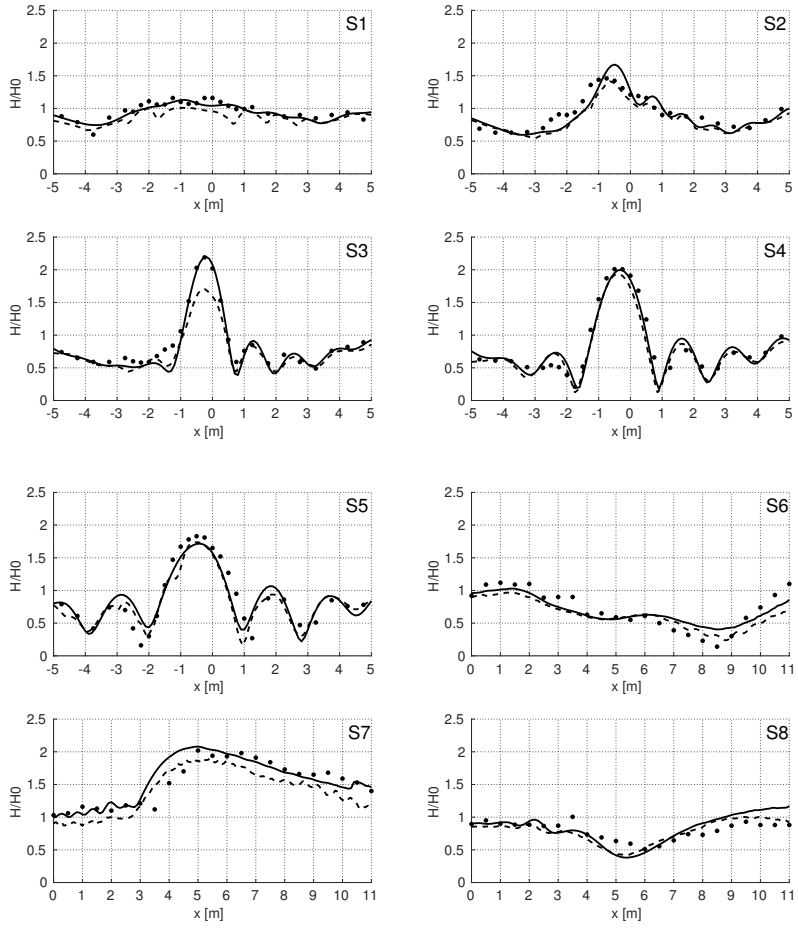

Fig. 2. Graphs showing comparison with results on wave height along various sections; present work numerical (—); experimental [15] (•), FUNWAVE 1.0 numerical [16] (- -)

accurately estimate the transmission coefficient for all cases in H/h range of 0.1 to 0.35. Reflection coefficient is predicted well for low H/h but is over-predicted for higher H/h. This is possibly because the model is linearly dispersive and with increase in wave-height, the non-linearity of the solitary wave increases leading to modelling errors. The turbulence modelling done in the present work is based on depth integrated properties and hence cannot include the effects of eddies formed along the depth. This is supported by the observation stated in [17], according to which surface wave models tend to over estimate reflection from porous structure due to improper turbulence modelling.

4.3 Study of Ship Motion in Narrow Channel

This numerical experiment presents a possible extension of this model. Inland waterways, in form of river, canals, backwaters and creeks are utilised for freight transport at low cost.

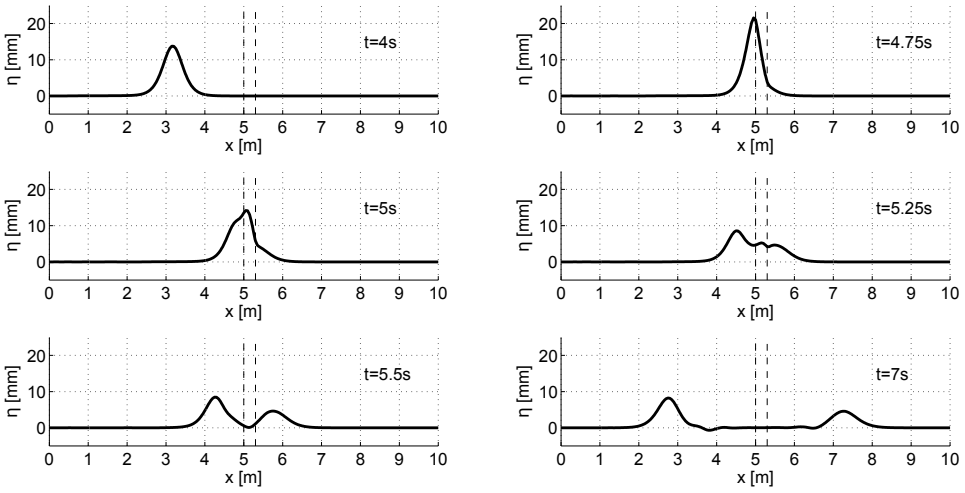

Fig. 3. Snapshots of surface elevation at different time instants depicting splitting of solitary wave through the porous breakwater

The long waves generated by the motion of cargo vessels in these narrow channels can cause damage to the river banks and surrounding region through erosion. There is a need to study this interaction between ship-generated waves and river-bank along the navigation length.

A river-bank can be simplified as a partially reflecting wall, similar to a porous breakwater. The characteristics of river-bank are tuned using stone size and porosity parameters. The ship waves are generated using moving pressure field based on the formulation of [18]. This approach can be used to study the interaction over long navigation channels.

The schematic describing numerical setup for a parametric example study is shown in Fig 5. A narrow channel of width $23m$ has a porous bank, denoted by lines P1 and P2. The width of each porous region is $5m$. Water depth is $2.5m$ in the entire region. A slender vessel of length $L = 5m$, width $B = 1m$ and draft $T = 0.2m$, is moved along midline of this channel at a constant speed corresponding to $Fr_d = 0.7$. The moving pressure field with respect to centre of ship is given by

$$p(x, y) = p_0 \left[1 - c_L(x/L)^4\right] \left[1 - c_B(y/B)^2\right] \exp\left[-a(y/B)^2\right] \tag{9}$$

with peak pressure $p_0 = \rho g T$, and shape constants $a = 16$, $c_b = 2$, $c_l = 16$.

The computational domain is $100m \times 43m$. The ship moves along the centre line. Therefore, to successfully capture the sharp gradient of the moving pressure field, the region between $y = 20m$ and $y = 23m$ is meshed with mean element area $0.02m^2$, and the remaining region with mean element area $0.08m^2$. A $5m$ wide sponge layer is placed at each boundary. This gives a mesh with 70398 elements, 35570 linear nodes and 141537 total nodes. Time step is $0.01s$.

Wave elevation is measured along a line parallel to the bank at a distance of $1m$ as denoted by M1. Porosity and stone size are two parameters that can be adjusted for the bank. For this study, the stone size is kept constant at $20cm$. Three values of porosity, 15%, 30% and 50%, are tested. Fig 6 shows the wave elevation measurement on M1 at $25s$ for these three porosities. The measured maximum wave height for the three porosities

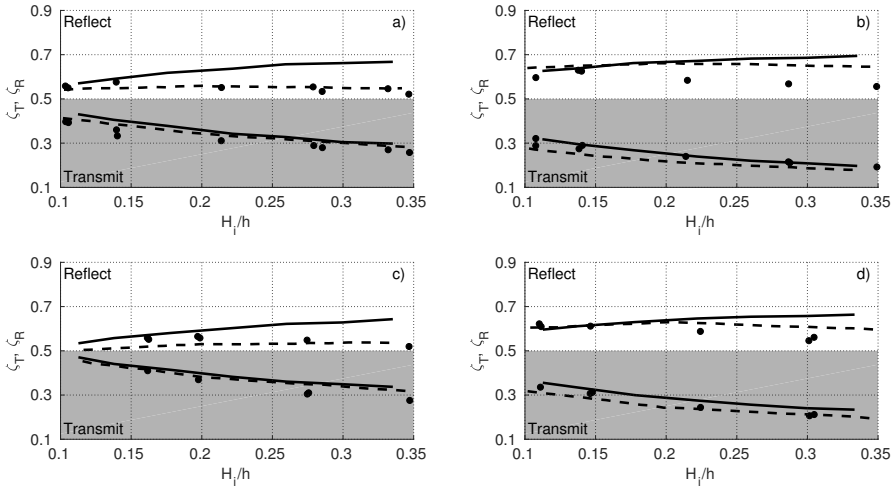

Fig. 4. Graphs showing estimated transmission and reflection coefficient for 1D solitary waves through porous breakwater; Shaded region shows transmission; a) $s = 1.6cm$ $b = 15cm$; b) $s = 1.6cm$ $b = 30cm$; c) $s = 2.0cm$ $b = 15cm$; d) $s = 2.0cm$ $b = 30cm$; present work (——); referred numerical [7] (- -); experimental [7] (•)

values is $0.0934m$, $0.0819m$ and $0.0705m$ respectively. The wave height measurement and the wave train in Fig 6 show a reduction in reflection from the bank with increasing porosity value. The magnitude of wave height can be used to estimate erosion at river bank. Due to the unstructured mesh formulation, the channel shape is not limited to rectangles. This approach can be used to study curved channels too.

5 Conclusion

This manuscript presented a numerical model of Boussinesq equations incorporating flow through porous structures. The version of equations used was capable of simulating waves transformation process in shallow to intermediate water depths. The model uses porous flow equations derived based on Darcy velocity with laminar and turbulent drag resistance terms.

The finite element formulation was done using standard Galerkin method. The spatial interpolation of water elevation and auxiliary variable were done using linear polynomial, and a quadratic shape function was used for depth integrated velocities. The domain integrals were calculated analytically for standard triangle and scaled using the Jacobian, which improves accuracy and efficiency.

The basic wave model was tested using standard Berkhoff shoal experiment. The wave height was measured along pre-defined lines and compared with the experiment results with acceptable accuracy.

Numerical formulation of porous flow was validated using interaction of solitary wave with porous breakwater. The tuning coefficients for laminar and turbulent resistance terms were obtained by minimising error in transmission and reflection coefficient. The tuned model was tested for various stone sizes and breakwater widths with constant porosity.

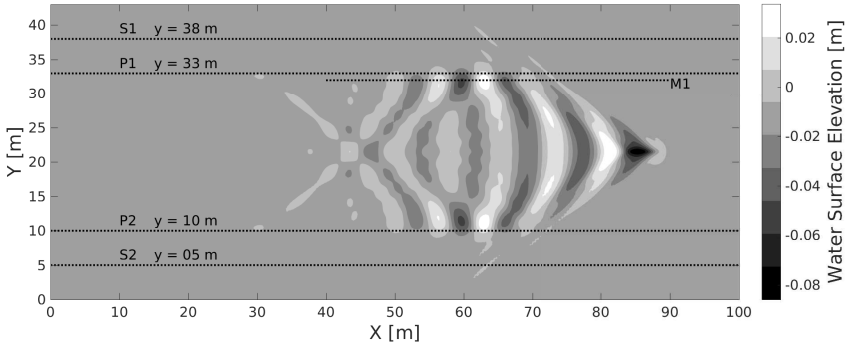

Fig. 5. Schematic for numerical experiment setup and contour plot of water elevation at $22s$ for $\lambda = 0.15$

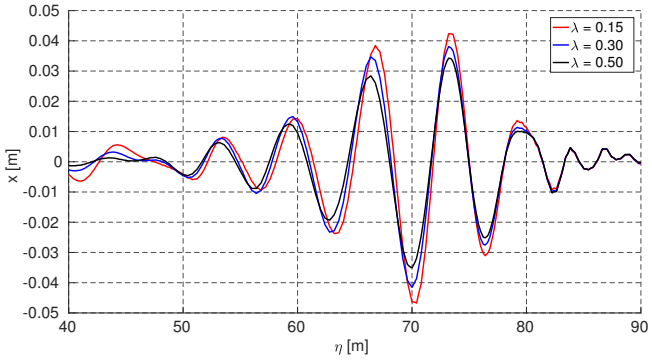

Fig. 6. Graph shown surface elevation at $25s$ along M1 for three different porosities

The results of transmission coefficient show good agreement with experiment in every test case with the same set of empirical constants. Reflection coefficient was found to be over-estimated with increasing non-linearity of incident wave.

The application of model was demonstrated through study of interaction of ship generated waves with porous walls in a narrow channel. Porosity of the walls of constant depth channel was varied and wave train formed by interaction of incident and partially reflected wave was measured near the wall. The trend of decreasing wave height with increasing wall porosity was obtained and their values for the specific ship characteristics were presented.

This manuscript reported the development and validation of the new numerical model. The potential real world application of the model was exhibited for both off-shore and inland waterways problems.

References

1. Per A. Madsen and Ole R. Sørensen. A new form of the Boussinesq equations with improved linear dispersion characteristics. Part 2. A slowly-varying bathymetry. *Coastal Engineering*, 18(3-4):183–204, 1992.

2. Ge Wei, James T. Kirby, Stephan T. Grilli, and Ravishankar Subramanya. A fully nonlinear Boussinesq model for surface waves. Part 1. Highly nonlinear unsteady waves. *Journal of Fluid Mechanics*, 294:71, 1995.
3. P. a. Madsen, H. B. Bingham, and Hua Liu. A new Boussinesq method for fully nonlinear waves from shallow to deep water. *Journal of Fluid Mechanics*, 462:1–30, 2002.
4. S. A.S.A. Karunarathna and Pengzhi Lin. Numerical simulation of wave damping over porous seabeds. *Coastal Engineering*, 53(10):845–855, 2006.
5. H.F. Burcharth and O.K. Andersen. On the one-dimensional steady and unsteady porous flow equations. *Coastal Engineering*, 24(3-4):233–257, mar 1995.
6. Xiping Yu and Hiroyoshi Togashi. Combined Diffraction and Transmission of Water Waves around a Porous Breakwater Gap. In *Coastal Engineering 1996*, pages 2063–2076, New York, NY, aug 1997. American Society of Civil Engineers.
7. Patrick J Lynett, Philip L Liu, Inigo J Losada, and Cesar Vidal. Solitary Wave Interaction with Porous Breakwaters. *Journal of Waterway, Port, Coastal, and Ocean Engineering*, 126(6):314–322, 2000.
8. Seung-Buhm Woo and Philip L.-F. Liu. Finite-Element Model for Modified Boussinesq Equations. II: Applications to Nonlinear Harbor Oscillations. *Journal of Waterway, Port, Coastal, and Ocean Engineering*, 130(1):17–28, jan 2004.
9. L. Pinheiro, C.J. Fortes, J.A. Santos, and M. Walkley. Implementation of partial reflection boundary conditions in wave propagation model BOUSSIIW. *Journal of Coastal Research*, SI 56:1040–1044, 2009.
10. Ole R. Sørensen, Hemming A. Schäffer, and Lars S. Sørensen. Boussinesq-type modelling using an unstructured finite element technique. *Coastal Engineering*, 50(4):181–198, 2004.
11. Frank. Engelund. *On the laminar and turbulent flows of ground water through homogeneous sand.* Akademiet for de tekniske videnskaber, 1953.
12. PARALUTION Labs. Paralution v1.1.0, 2016.
13. G. R. Liu and Y. T. Gu. *An introduction to meshfree methods and their programming.* Springer Netherlands, 2005.
14. James T. Kirby and Robert A Dalrymple. Verification of a parabolic equation for propagation of weakly-nonlinear waves. *Coastal Engineering*, 8(3):219–232, aug 1984.
15. J. C W Berkhoff, N. Booy, and A. C. Radder. Verification of numerical wave propagation models for simple harmonic linear water waves. *Coastal Engineering*, 6(3):255–279, 1982.
16. James T Kirby, Ge Wei, Qin Chen, Andrew B Kennedy, and Robert A Dalrymple. FUNWAVE 1.0. Fully nonlinear Boussinesq wave model. Documentation and user's manual. Technical report, University of Delaware, Newark, 1998.
17. S.A. Hughes. *Physical Models and Laboratory Techniques in Coastal Engineering*, volume 7. 1993.
18. D. Bayraktar Ersan and S. Beji. Numerical simulation of waves generated by a moving pressure field. *Ocean Engineering*, 59, 2013.